

Received March 17, 2021, accepted April 26, 2021, date of publication May 6, 2021, date of current version May 18, 2021.

Digital Object Identifier 10.1109/ACCESS.2021.3077978

Experimental and Numerical Investigation of the Shock Wave Induced by a High-Pressure Diesel Spray

YUE LI¹, BINGBIN LIU¹, MINGYU WANG¹, GANG LIU¹, AND QUAN DONG²

¹College of Navigation, Shandong Jiaotong University, Weihai 264200, China

²Institute of Power and Energy Engineering, Harbin Engineering University, Harbin 150001, China

Corresponding author: Bingbing Liu (222012@sdjtu.edu.cn)

This work was supported in part by the National Natural Science Foundation of China under Grant 51406040 and Grant 51879056, in part by the Shandong Jiaotong Natural Science Foundation under Grant Z201939, in part by the Shandong Jiaotong University Doctoral Research Initiation Fund under Grant BS201902054 and Grant BS2018007, and in part by the Shandong Jiaotong University “Climbing” Research Innovation Team Program under Grant SDJTUC1802.

ABSTRACT The shock wave phenomenon has been very common in the high-pressure fuel spray. In this paper, the effect of the shock waves on the spray development and the variations of the flow field parameters were investigated using the Schlieren imaging coupled with a numerical simulation. Results showed that the shock wave contributed to the increase in the spray tip penetration. The mixing characteristics of the spray also improved in the shock-wave state. Numerical simulations were used to investigate the flow characteristics of the shock wave and the effect of the shock wave on the flow field parameters. Results showed that the simulated shock wave characteristic parameters were consistent with the experimental data. In addition, the flow field parameters were affected by the shock wave propagation. The maximum density ratio, pressure ratio and temperature ratio after and before the shock wave are 2.46, 2.01 and 1.15, respectively, under the fuel injection pressure of 320MPa.

INDEX TERMS Diesel spray, shock wave, propagation characteristic, numerical simulation, Schlieren imaging.

I. INTRODUCTION

To meet the stringent emission regulations, a high pressure fuel injection pressure is considered to be an effective means to improve the combustion and emission performance of an engine [1]–[3]. With the continuous increased injection pressure, the speed of the diesel spray at the nozzle exit increases. In addition, the application of pre-injection and the low temperature combustion technology produce a low sound speed. Therefore, the supersonic fuel spray becomes inevitable in a modern diesel engine [4]–[6]. Shock waves are generated around the spray when the spray is supersonic. It is considered that the atomization of the spray is affected by the shock wave propagation [7]–[9].

Researchers have studied the generation and propagation characteristics of the shock waves using modern testing technology [10]–[15]. In the early 1990s, Nakahira *et al.* first observed the shock waves during the fuel injection process

using the Schlieren imaging method. It was found that the shock wave has a positive effect on the spray breakup, and the detached shock wave propagates at the speed of sound [10]. MacPhee *et al.* pointed out that the gas density after the shock wave increased by 15% based on an X-ray technique [11]. Pianthong *et al.* set up an ultra-high pressure fuel injection device to study the types and propagation characteristics of the shock waves. The results showed that the Mach number of the jet determined the shock wave types [12]. Jia *et al.* found that the leading shock wave had two propagation modes under an ultra-high fuel injection pressure. In recent years, a numerical simulation was used to analyze the propagation behavior of the shock wave induced by the supersonic diesel spray [13]. Im *et al.* studied the dynamic behaviors of shock waves using numerical simulation. It was found that the shock wave caused a complex gas disturbance around the spray [14]. Quan *et al.* studied the interaction between the shock wave and the spray, and the simulation results were in good agreement with the experiments [15].

The associate editor coordinating the review of this manuscript and approving it for publication was Chaitanya U. Kshirsagar.

The effect of shock waves on the development of the fuel spray was further studied in recent years [16]–[21]. Pianthong and Milton *et al.* found that the propagation of the shock waves contributed to the diffusion and combustion of the spray [16]. Payri *et al.* investigated the evolution of the spray macroscopic structures in N2 and SF6 environments. It was found that the shock wave promoted the development of the spray tip penetration. Shock waves lead to a 6% increase in the spray tip penetration [17]. Furthermore, the effect of shock waves on the mixing characteristic of the spray was analyzed by Song *et al.* The results showed that the shock waves promote the mixing effect of the spray [18]. Jia *et al.* found that increasing the fuel injection pressure had a positive effect on the spray atomization [19]. Huang *et al.* proposed a prediction model of the jet tip penetration considering the shock wave. The simulation results are consistent with the experimental data [20], [21].

However, previous studies have mainly focused on the generation and propagation characteristics of the shock waves. The characteristics of shock waves induced by supersonic fuel injection and the control mechanism of shock wave in the cylinder are still unclear, which has become an urgent problem to be solved in the optimization of the fuel injection system. At present, it is considered that the generation and propagation of the shock wave affect the breakup and development of the spray, but the impact degree has not been fully grasped. Therefore, the influence of the shock wave on the spray development is needed for further research. In addition, the effect of the shock wave on the flow field parameters in the cylinder has rarely been investigated. Based on the above analysis, this paper investigated the evolution of the supersonic fuel spray and the induced shock wave using the Schlieren imaging and numerical simulation. The present paper has three objectives: (1) Analyze the spray development and mixing characteristic in the shock-wave state, (2) Understand the variations of the flow field parameters under different fuel injection pressures during shock wave propagation, and (3) Study the flow characteristics of the shock wave using large eddy simulations.

II. EXPERIMENTAL METHOD

The experimental setup is shown in Fig. 1. The Schlieren technique determines the density gradient in the flow field. It is suitable for capturing the spray profiles and the shock waves. The detailed experimental setup information has been described in a previous publication [18].

The shock wave angle and shock wave penetration of oblique shock wave are indicated in Figure 2. The temperature of the experiment is 298K. The fuel injection pressure is set from 60MPa to 160MPa.

III. NUMERICAL APPROACH

A. NUMERICAL METHODOLOGY

The governing equations for the simulation involve the conservation of mass, momentum, energy and species.

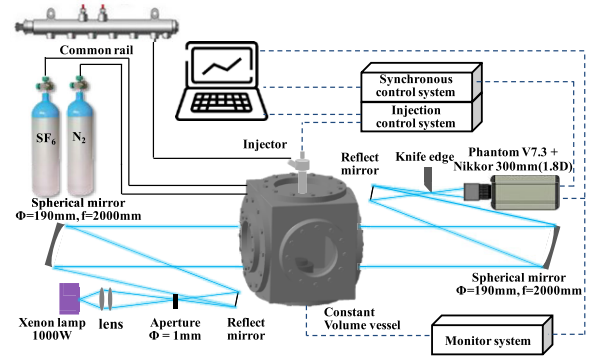


FIGURE 1. Schematic diagram of experimental setup.

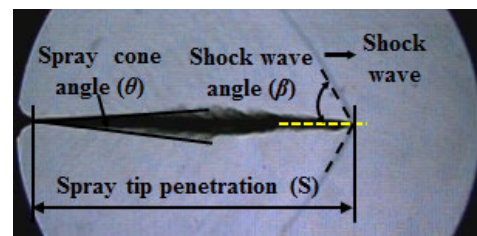


FIGURE 2. Definition of shock wave characteristic parameters.

The equations are listed below.

$$\frac{\partial \rho}{\partial t} + \frac{\partial \rho u_i}{\partial x_i} = s \quad (1)$$

$$\frac{\partial \rho u_i}{\partial t} + \frac{\partial \rho u_i u_j}{\partial x_j} = -\frac{\partial P}{\partial t} + \frac{\partial \sigma_{ij}}{\partial x_j} + s_i \quad (2)$$

$$\begin{aligned} \frac{\partial \rho e}{\partial t} + \frac{\partial \rho u_i e}{\partial x_i} = & -P \frac{\partial u_i}{\partial x_i} + \sigma_{ij} \frac{\partial u_i}{\partial x_j} + \frac{\partial}{\partial x_i} \left(k \frac{\partial T}{\partial x_i} \right) \\ & + \frac{\partial}{\partial x_i} \left(\rho \sum_m D h_m \right) \frac{\partial Y_m}{\partial x_i} + s \end{aligned} \quad (3)$$

$$\frac{\partial \rho_m}{\partial t} + \frac{\partial \rho_m u_i}{\partial x_i} = \frac{\partial}{\partial x_i} \left(\rho D \frac{\partial Y_m}{\partial x_i} \right) + s_m \quad (4)$$

where ρ , u , P and T are, respectively, the density, velocity, pressure and temperature of the mixture, ρ_m is the density of species m , σ_{ij} is the viscous stress tensor, s_m is the source term, D is the mass diffusion coefficient, e is the specific internal energy, Y_m is the mass fraction of species m , k is the conductivity, and h_m is the species enthalpy.

In the simulation, the Volume of Fluid (VOF) method is used to simulate the spray and the shock wave. This is because the VOF method is a numerical technique used to locate and track the free surface in the flow field [15]. Both the liquid and gas flow are assumed to be compressible. The parameter α represents the void fraction of a cell, which is presented as (5)

$$\alpha = \frac{m_g / \rho_g}{m_g / \rho_g + m_l / \rho_l} \quad (5)$$

where the subscripts g and l represent the gas phase and the liquid phase, respectively, m is the total mass fraction, ρ is

the density in the cell. $\alpha = 0$ represents the cell containing only liquid, $0 < \alpha < 1$ represents the cell containing both a liquid and gas and $\alpha = 1$ represents the cell containing only gas. The global density is presented as (6)

$$\rho = \alpha\rho_g + (1 - \alpha)\rho_l \quad (6)$$

The Pressure Implicit with Splitting of Operators (PISO) Algorithm was used to solve the conservation of mass and momentum equations. The energy and the species equations can also be solved after the calculations of the momentum and pressure have been completed.

B. SIMULATION SETUP AND VALIDATION

The simulation geometry and the grid setting are shown in Fig. 3. The simulations were carried out in a wall-bound closed system. The system contains a high-pressure fuel tank (P_{inj}) and a low-pressure ambient gas tank (P_b) at $P_b = 0.1\text{MPa}$. The initial gas temperature (T_b) remained constant at $T_b = 300\text{K}$. D is the diameter of the injector, which is 0.14mm . The five simulated fuel injection pressures were $P_0 = 120, 140, 160, 240$ and 320MPa .

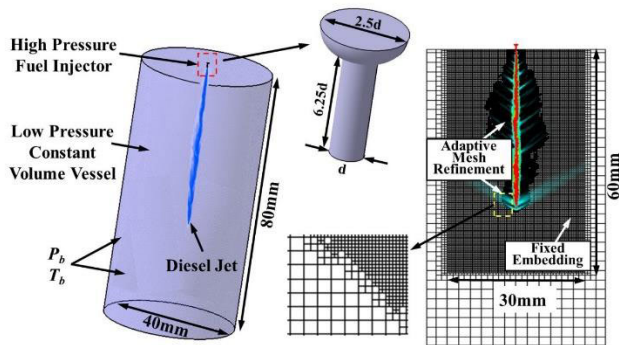


FIGURE 3. The simulation geometry and the grid settings.

The computational domain is a cylindrical box with the diameter of 30mm and the height of 80mm . Adaptive Mesh Refinement (AMR) was used to generate the highly refined grid to accurately and precisely simulate the high-pressure diesel spray and the shock wave phenomenon. Large eddy simulation (LES) was used as the turbulence model to capture the liquid and gas flow states. The simulation was carried out in CONVERGE software. In this paper, the hexahedral grid was used. The base grid size is $2.56 \times 10^{-3}\text{m}$. The fixed embedding grid scale is 3 and the grid size is $3.2 \times 10^{-4}\text{m}$. AMR was used to capture the high density gradient gas interface and the grid scale is 5. The minimum grid size is $8 \times 10^{-5}\text{m}$. The total number of grids is 7 million.

C. MODEL VALIDATION

The visualization experimental data were used to verify the simulation calculation accuracy. The simulation results and the visualization images are shown in Fig. 4 and Fig. 5. The fuel injection pressure was 120MPa , 140MPa and 160MPa , and the ambient pressure was 0.1MPa . It can be seen from

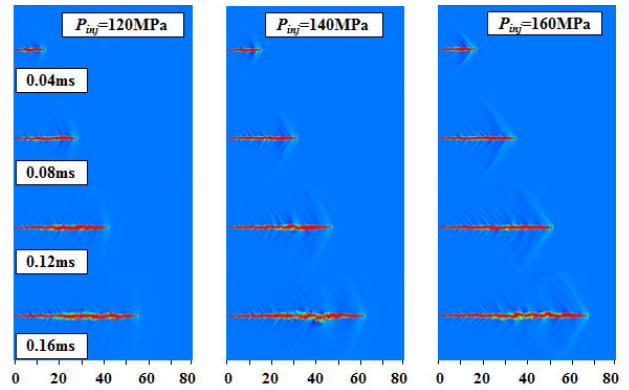


FIGURE 4. Simulation of the spray and shock wave.

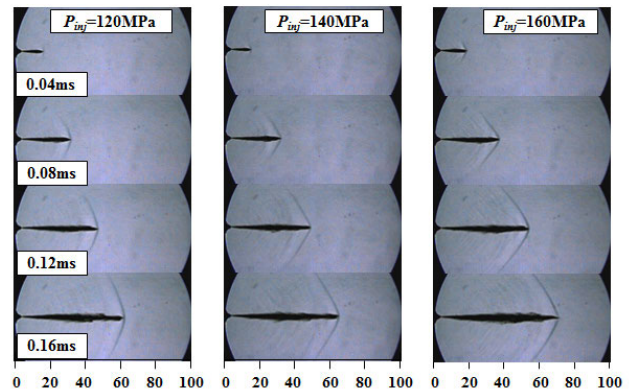


FIGURE 5. Visualization images of the spray and shock wave.

the figure that the simulation of the spray and the shock wave are in good agreement with the Schlieren images. The comparison of the spray and the shock wave parameters are analyzed below.

simulation geometry and the grid setting are shown in Fig. 3. The simulations were carried out in a wall-bound closed system. The system contains a high-pressure fuel tank (P_{inj}) and a low-pressure ambient gas tank (P_b) at $P_b = 0.1\text{MPa}$. The initial gas temperature (T_b) remained constant at $T_b = 300\text{K}$. D is the diameter of the injector, which is 0.14mm . The five simulated fuel injection pressures were $P_0 = 120, 140, 160, 240$ and 320MPa .

The comparison of the spray tip penetration and the shock wave angle are shown in Fig. 6. As shown in Fig. 6(a), the simulation spray tip penetration at the time of 0.16ms after the start of the injection ($ASOI$) is 55.40mm , 58.83mm and 64.07mm at the fuel injection pressures of 120MPa , 140MPa and 160MPa , respectively. The corresponding experimental data are 53.55mm , 56.93mm and 61.02mm . The maximum error of the spray tip penetration for the different fuel injection pressures is 5.1% . The comparison of the shock wave angle at the different fuel injection pressures is shown in Fig. 6(b). The maximum error of the shock wave is 3.3% . It can be seen that the simulation results are consistent with the experimental results. The simulation can be used

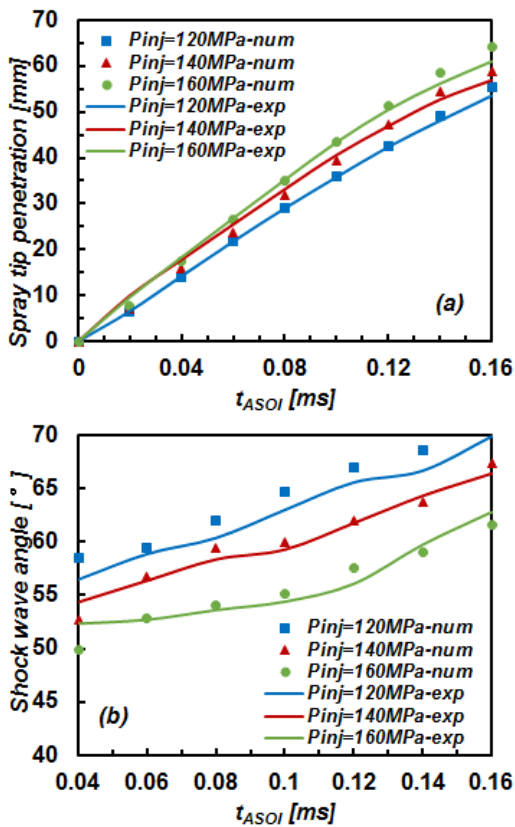


FIGURE 6. The comparison of the characteristic parameters between the experiment and simulation.

to analyze the effect of the shock waves on the flow field parameters.

IV. RESULTS AND DISCUSSION

A. EXPERIMENTAL RESULTS

The effect of shock wave on the spray macroscopic structure are shown in Fig. 7. The evolution of the spray and shock wave in the SF₆ gas are shown in Fig. 7(a) and Fig. 7(c). The images in the N₂ environment under the same injection condition are presented in Fig. 7(b) and Fig. 7(d). The fuel injection pressures are 60MPa and 140MPa respectively. Detailed experimental conditions are listed in the previous literature [18].

The effect of shock wave on the macroscopic structure of the spray are shown in Fig. 8. It can be seen that the shock wave promotes the spray tip penetration development. But it is worth noting that the shock wave has an opposite effect on spray tip penetration before $t_{ASOI} = 0.1$ ms. This is because the generation of the shock waves consumes the spray energy. The increased gas density after the shock wave also inhibits the development of the spray. The result shows that the shock wave contributes to the development of the spray.

Fig. 9 shows the entrained gas quantity and the spray average equivalent ratio curves when $P_{inj} = 60$ MPa. As shown in Fig. 9, the shock wave (SW) promotes the air entrainment quantity. This is because the shock wave carries energy.

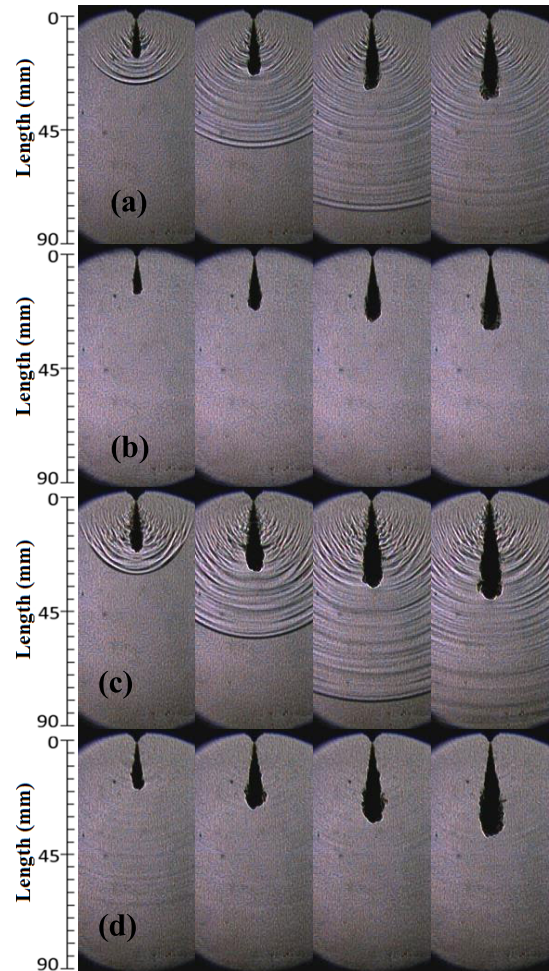


FIGURE 7. Evolution of the spray macroscopic structure.

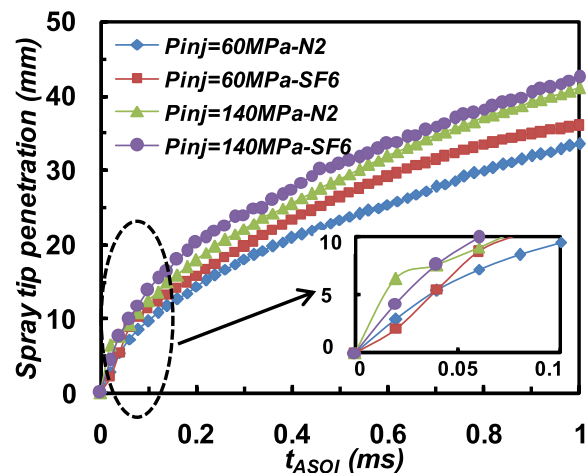


FIGURE 8. Comparison of the spray tip penetration.

The turbulence in the cylinder increases with the spread of the shock waves. The average equivalent ratio in the shock-wave state is 35.1% lower than that in the non-shock-wave state at $t_{ASOI} = 0.2$ ms. The curves presents that the shock wave

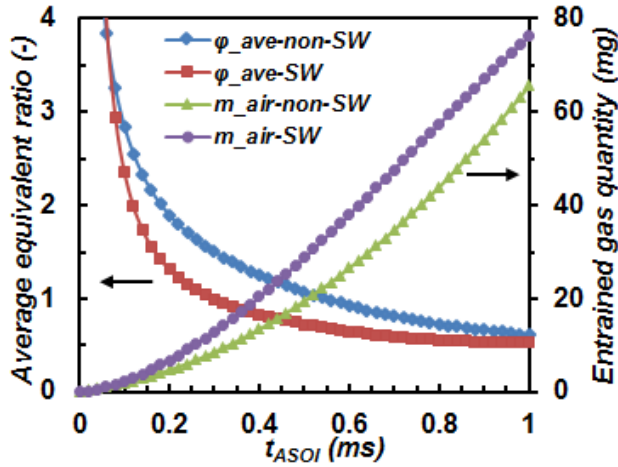


FIGURE 9. Comparison of the air entrainment quantity and the average equivalence ratio.

improves the mixing effect of the spray, which improves the combustion and emission performance of the engine.

B. NUMERICAL RESULTS

The effect of the shock wave on the variations of the flow field parameters in the shock-wave state was simulated based on the validated simulation model. The fuel injection pressures are 240MPa and 320MPa. The simulation results are shown in Fig. 10.

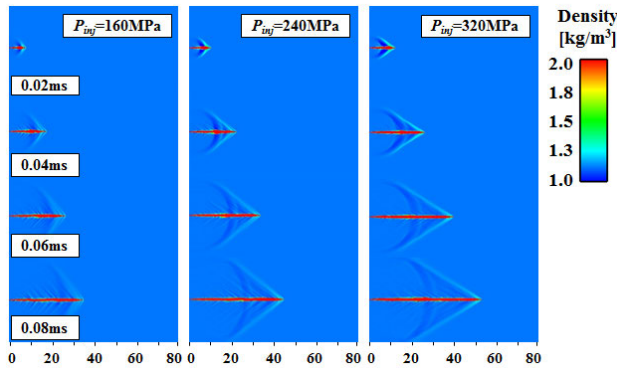


FIGURE 10. Simulation results of the induced shock wave.

Seventeen sampling points were selected on the shock wave surface to study the variations of the flow field parameters. The selected sampling points are shown in Fig. 11. The flow field parameters before and after the shock wave are analyzed below.

A direct comparison of the variations in the temperature and the density at the shock wave surface at the fuel injection pressures of 240MPa and 320MPa is shown in Fig. 12. It can be seen that the impact of the shock wave on the flow field parameter is different at the different positions. For the position at the top of the spray, the high temperature gradient and

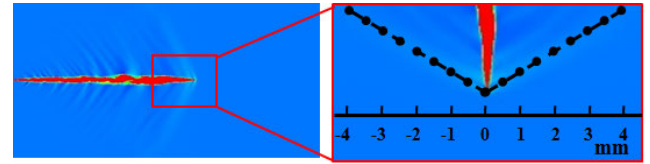


FIGURE 11. Spatial distribution of the sampling point on the shock wave surface.

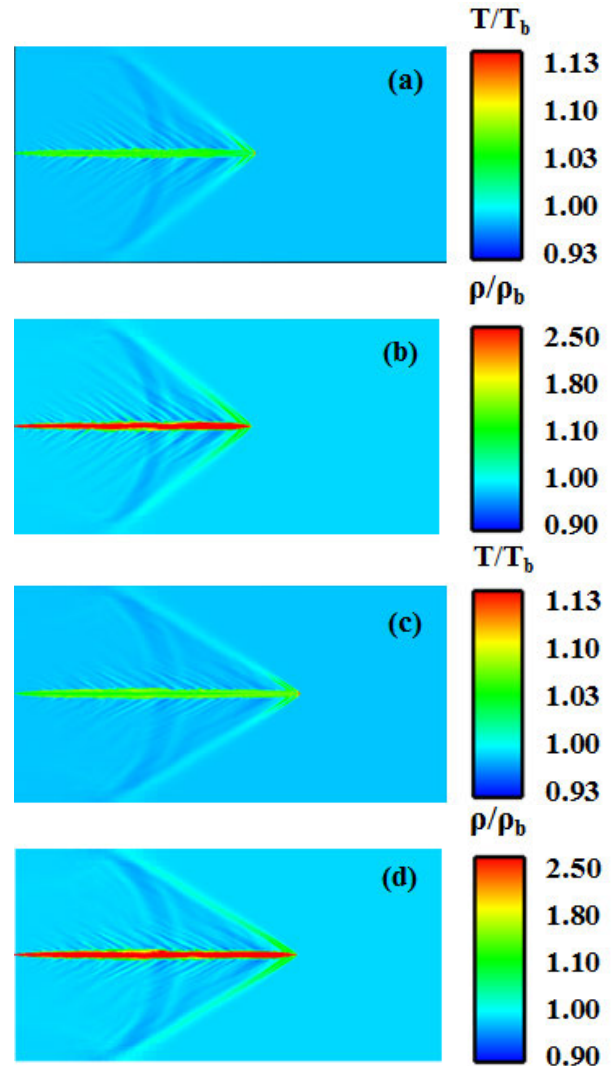


FIGURE 12. Effect of shock wave on temperature and density field.

density gradient are caused by the shock wave. The impact on the parameters becomes small on the outside of the shock wave surface. In addition, there is a low density area behind the leading edge shock. This explains why the shock wave promotes the development of the spray tip penetration.

Figure 13 indicates the variations of the density field, pressure field and temperature field at $t_{ASOT} = 0.08ms$. The subscripts 1 and 2 represent the parameter before and after the shock wave, respectively. The pressure, density and temperature ratio distributions are similar. $P_2/P_1, \rho_2/\rho_1$

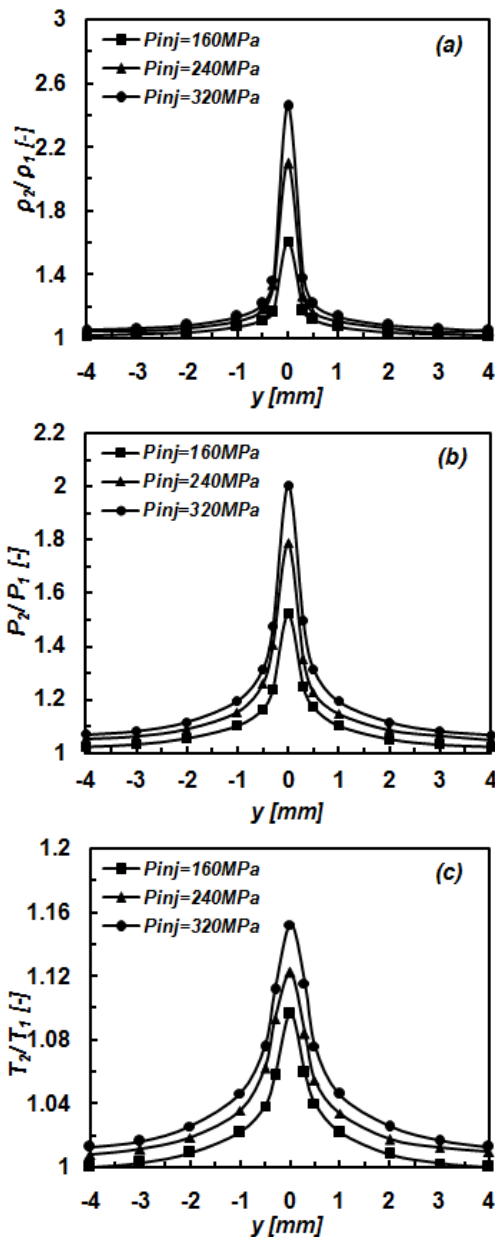


FIGURE 13. Variations in flow field parameters on the shock wave surface.

and T_2/T_1 have the highest values at the central position of the shock wave. This is because the shock wave at the center position can be considered as the normal shock wave. The ratios of the flow parameters decrease from the center to both sides. The maximum density ratio, pressure ratio and temperature ratio are, respectively, 2.46, 2.01 and 1.15 at $P_{inj} = 320$ MPa. The maximum density ratio, pressure ratio and temperature ratio at the fuel injection pressure of 320 MPa are 52.9%, 31.7% and 5% higher than those for the fuel injection pressure of 160 MPa. The results indicate that the shock wave can increase the temperature in the cylinder, which can shorten the fuel ignition delay period and improve the ignition characteristic. The increase in the density behind

the shock wave will suppress the increase of the spray tip penetration as mentioned above. This result is consistent with the experimental result in Fig. 8. In addition, the pressure disturbance promotes the spray mixing effect as shown in Fig. 9.

V. CONCLUSION

In this paper, the effect of the shock waves on the spray development and the variations of the flow field parameters were investigated using the Schlieren imaging coupled with a numerical simulation. The experimental results indicate that the macroscopic structure and the mixing of the spray improves with the action of shock wave. The impact of shock wave on the spray atomization in the cylinder should be considered in the design of the fuel injection system. The numerical results presents that the maximum density ratio, pressure ratio and temperature ratio are, respectively, 2.46, 2.01 and 1.15 at $P_{inj} = 320$ MPa. The maximum density ratio, pressure ratio and temperature ratio at the fuel injection pressure of 320 MPa are 52.9%, 31.7% and 5% higher than those for the fuel injection pressure of 160 MPa. The variations of the parameters are directly related to the spray development and the mixing effect.

REFERENCES

- [1] G. Li, Z. Liu, T. H. Lee, C. F. Lee, and C. Zhang, "Effects of dilute gas on combustion and emission characteristics of a common-rail diesel engine fueled with isopropanol-butanol-ethanol and diesel blends," *Energy Convers. Manage.*, vol. 165, pp. 373–381, Jun. 2018, doi: 10.1016/j.enconman.2018.03.073.
- [2] S. Imtenan, S. M. A. Rahman, H. H. Masjuki, M. Varman, and M. A. Kalam, "Effect of dynamic injection pressure on performance, emission and combustion characteristics of a compression ignition engine," *Renew. Sustain. Energy Rev.*, vol. 52, pp. 1205–1211, Dec. 2015, doi: 10.1016/j.rser.2015.07.166.
- [3] O. A. Kuti, J. Zhu, K. Nishida, X. Wang, and Z. Huang, "Characterization of spray and combustion processes of biodiesel fuel injected by diesel engine common rail system," *Fuel*, vol. 104, pp. 838–846, Feb. 2013, doi: 10.1016/j.fuel.2012.05.014.
- [4] W. E. Eagle, S. B. Morris, and M. S. Wooldridge, "High-speed imaging of transient diesel spray behavior during high pressure injection of a multi-hole fuel injector," *Fuel*, vol. 116, pp. 299–309, Jan. 2014.
- [5] S. H. Park, H. J. Kim, and C. S. Lee, "Effect of multiple injection strategies on combustion and emission characteristics in a diesel engine," *Energy Fuels*, vol. 30, pp. 810–818, Jan. 2016, doi: 10.1021/acs.energyfuels.5b02121.
- [6] K. Mathivanan, J. M. Mallikarjuna, and A. Ramesh, "Influence of multiple fuel injection strategies on performance and combustion characteristics of a diesel fuelled HCCI engine—An experimental investigation," *Exp. Thermal Fluid Sci.*, vol. 77, pp. 337–346, Oct. 2016, doi: 10.1016/j.expthermflusci.2016.05.010.
- [7] T.-M. Jia, Y.-S. Yu, and G.-X. Li, "Experimental investigation of effects of super high injection pressure on diesel spray and induced shock waves characteristics," *Exp. Thermal Fluid Sci.*, vol. 85, pp. 399–408, Jul. 2017, doi: 10.1016/j.expthermflusci.2017.03.026.
- [8] S. Zakrzewski, B. E. Milton, K. Pianthong, and M. Behnia, "Supersonic liquid fuel jets injected into quiescent air," *Int. J. Heat Fluid Flow*, vol. 25, no. 5, pp. 833–840, Oct. 2004, doi: 10.1016/j.ijheatfluidflow.2004.05.010.
- [9] L. M. Pickett and S. Kook, "Effect of ambient temperature and density on shock wave generation in a diesel engine," *Atomization Sprays*, vol. 20, no. 2, pp. 163–175, 2010, doi: 10.1615/atomizspr.v20.i2.50.
- [10] T. Nakahira, M. Komori, M. Nishida, and K. Tsujimura, "The shock wave generation around the diesel fuel spray with high pressure injection," in *Proc. SAE Tech. Paper*, Apr. 1992, pp. 741–746, doi: 10.4271/920460.
- [11] A. G. MacPhee, "X-ray imaging of shock waves generated by high-pressure fuel sprays," *Science*, vol. 295, no. 5558, pp. 1261–1263, Feb. 2002, doi: 10.1126/science.1068149.

- [12] K. Piantong, A. Matthujak, K. Takayama, B. E. Milton, and M. Behnia, "Dynamic characteristics of pulsed supersonic fuel sprays," *Shock Waves*, vol. 18, no. 1, pp. 1–10, Jun. 2008, doi: [10.1007/s00193-008-0123-4](https://doi.org/10.1007/s00193-008-0123-4).
- [13] T.-M. Jia, G.-X. Li, Y.-S. Yu, and Y.-J. Xu, "Effects of ultra-high injection pressure on penetration characteristics of diesel spray and a two-mode leading edge shock wave," *Exp. Thermal Fluid Sci.*, vol. 79, pp. 126–133, Dec. 2016, doi: [10.1016/j.expthermflusci.2016.07.006](https://doi.org/10.1016/j.expthermflusci.2016.07.006).
- [14] K.-S. Im, S.-K. Cheong, X. Liu, J. Wang, M.-C. Lai, M. W. Tate, A. Ercan, M. J. Renzi, D. R. Schuette, and S. M. Gruner, "Interaction between supersonic disintegrating liquid jets and their shock waves," *Phys. Rev. Lett.*, vol. 102, no. 7, pp. 1–4, Feb. 2009, doi: [10.1103/physrevlett.102.074501](https://doi.org/10.1103/physrevlett.102.074501).
- [15] S. Quan, M. Dai, E. Pomraning, P. K. Senecal, K. Richards, S. Som, S. Skeen, J. Manin, and L. M. Pickett, "Numerical simulations of supersonic diesel spray injection and the induced shock waves," *SAE Int. J. Engines*, vol. 7, no. 2, pp. 1054–1060, Apr. 2014, doi: [10.4271/2014-01-1423](https://doi.org/10.4271/2014-01-1423).
- [16] B. E. Milton and K. Piantong, "Pulsed, supersonic fuel jets—A review of their characteristics and potential for fuel injection," *Int. J. Heat Fluid Flow*, vol. 26, no. 4, pp. 656–671, Aug. 2005, doi: [10.1016/j.ijheatfluidflow.2005.03.002](https://doi.org/10.1016/j.ijheatfluidflow.2005.03.002).
- [17] J. M. Desantes, R. Payri, F. J. Salvador, and V. Soare, "Study of the influence of geometrical and injection parameters on diesel sprays characteristics in isothermal conditions," in *Proc. SAE Tech. Paper*, 2005, pp. 1–12, doi: [10.4271/2005-01-0913](https://doi.org/10.4271/2005-01-0913).
- [18] E. Song, Y. Li, Q. Dong, L. Fan, C. Yao, and L. Yang, "Experimental research on the effect of shock wave on the evolution of high-pressure diesel spray," *Exp. Thermal Fluid Sci.*, vol. 93, pp. 235–241, May 2018, doi: [10.1016/j.expthermflusci.2018.01.004](https://doi.org/10.1016/j.expthermflusci.2018.01.004).
- [19] T.-M. Jia, G.-X. Li, Y.-S. Yu, and Y.-J. Xu, "Propagation characteristics of induced shock waves generated by diesel spray under ultra-high injection pressure," *Fuel*, vol. 180, pp. 521–528, Sep. 2016, doi: [10.1016/j.fuel.2016.04.009](https://doi.org/10.1016/j.fuel.2016.04.009).
- [20] W. Huang, Z. Wu, Y. Gao, Z. Li, and L. Li, "Shock wave generation and its influencing parameters based on diesel injector," *Chin. Sci. Bull.*, vol. 59, no. 27, pp. 3504–3510, Sep. 2014, doi: [10.1007/s11434-014-0431-2](https://doi.org/10.1007/s11434-014-0431-2).
- [21] W. Huang, Z. Wu, Y. Gao, and L. Zhang, "Effect of shock waves on the evolution of high-pressure fuel jets," *Appl. Energy*, vol. 159, pp. 442–448, Dec. 2015, doi: [10.1016/j.apenergy.2015.08.053](https://doi.org/10.1016/j.apenergy.2015.08.053).



YUE LI received the Ph.D. degree in marine engineering from Harbin Engineering University.

He is currently a Lecturer with Shandong Jiaotong University. His current research interests include spray and combustion visualization and engine performance research.



BINGBING LIU received the Ph.D. degree in marine engineering from Dalian Maritime University.

She is currently a Lecturer with Shandong Jiaotong University. Her research interests include spray combustion of internal combustion engines, numerical simulation of multiphase flow, and mathematical modeling of complex fluids.



MINGYU WANG received the Ph.D. degree in marine engineering from Dalian Maritime University.

He is currently a Professor with Shandong Jiaotong University. His main research interests include intelligent shipping, waste-free navigation zone, and pollution prevention of ships.

GANG LIU, photograph and biography not available at the time of publication.

QUAN DONG, photograph and biography not available at the time of publication.

• • •